ARTICLE

OBC
www.rsc.org/obc

# An *ortho*-palladated dimethylbenzylamine complex as a highly efficient turnover catalyst for the decomposition of P=S insecticides. Mechanistic studies of the methanolysis of some P=S-containing phosphorothioate triesters†

**Zhong-Lin Lu, Alexei A. Neverov and R. Stan Brown***

*Department of Chemistry, Queen's University, Kingston, Ontario, Canada K7L 3N6. E-mail: rsbrown@chem.queensu.ca; Fax: 613-533-6669; Tel: 613-533-2400*

***Received 23rd June 2005, Accepted 25th July 2005***
***First published as an Advance Article on the web 15th August 2005***

An *ortho*-palladated complex Pd(dmba)(py)(OTf) (**9**), or Pd(*N*,*N*-dimethylbenzylamine)(pyridine)-(trifluoromethanesulfonate), was synthesized and its solution properties in methanol studied as a function of $^{s}_{s}$pH. In neutral solution the triflate dissociates from the complex to give a dominant form Pd(dmba)(py)($HOCH_3$), and in acid the pyridine dissociates to give Pyr–$H^+$ and Pd(dmba)($HOCH_3$)($HOCH_3$). Under basic conditions, Pd(dmba)(py)($HOCH_3$) ionizes to give Pd(dmba)(py)($^-OCH_3$) from which the pyridine can dissociate to yield a mixture of a bis-methoxy-bridged dimer $(Pd(dmba)(^-OCH_3))_2$ (**15**-dimer), and its monomer Pd(dmba)($HOCH_3$)-($^-OCH_3$). Kinetic studies under buffered conditions reveal that **9** is an effective catalyst for the methanolysis of fenitrothion and other P=S pesticides. The active form of the catalyst is a basic one having one associated methoxide generated with an apparent $^{s}_{s}pK_a$ of 10.8. Analysis of the change in the UV/vis spectrum as a function of $^{s}_{s}$pH generates a spectrophotometric $^{s}_{s}pK_a$ of 10.8 ± 0.1. This catalytic system is shown to promote the methanolysis of fenitrothion (**3**), diazinon (**4**), quinalphos (**5**), coumaphos (**10**) and dichlofenthion (**11**) at 0.05 mol $dm^{-3}$ triethyl amine buffer, $^{s}_{s}$pH 10.8, 25 °C, under turnover conditions where the [phosphorothioate]/[**9**] ratio is 48.6, 13.4, 13.4, 18.6, and 48.6 respectively. In all cases, the products were derived from displacement of the leaving group by methoxide, the second-order turnover rate constants being 36.9, 0.45, 0.12, >146.7 and 44.3 $dm^3\ mol^{-1}\ s^{-1}$ respectively. An associative mechanism for the catalyzed methanolysis of the P=S pesticides is proposed where a transiently coordinated S=P substrate is intramolecularly attacked by the $Pd^{II}$-coordinated methoxide.

## Introduction

In a recent series of papers Kazankov, Ryabov and co-workers[1] reported studies of metallacycles such as **1** (M = Pt, Pd; X = Cl; Z = pyridine, DMSO) and **2** (M = Pt, Pd; X = Cl; Z = pyridine), and reported that the latter oximes are remarkably good catalysts for the hydrolysis of sulfur-containing organophosphate (OP) triesters of which the pesticides fenitrothion (**3**), diazinon (**4**) and quinalphos (**5**) are but three examples.

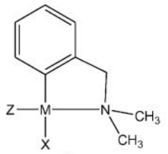

**1**

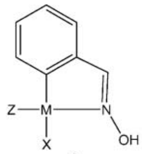

**2**

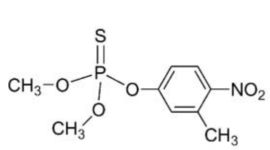

**3**

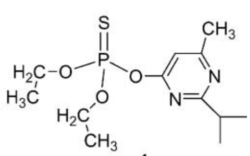

**4**

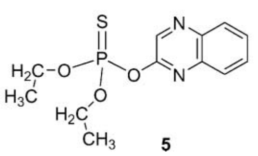

**5**

† Electronic supplementary information (ESI) available: X-ray crystallographic analysis reports for Pd(dmba)(py)(Cl) and Pd(dmba)(py)(OTf). See http://dx.doi.org/10.1039/b508917d

As part of an ongoing program to provide effective methods for the destruction of OP-based pesticides and chemical warfare agents,[2] we previously investigated $La^{3+}(^-OCH_3)$-catalyzed methanolysis of phosphate triesters such as paraoxon (**6**) and its phosphorothioate analogue (**7**)[2a–c] as well as the propensity of some aza complexes of $Zn^{2+}(^-OCH_3)$ and $Cu^{2+}(^-OCH_3)$ to catalyze the methanolysis of **6** and **3**.[2d] $La^{3+}$, being a 'hard' metal ion in the Pearson 'hard/soft' sense,[3] cannot promote the methanolysis of the P=S pesticides, but the somewhat 'softer' $Zn^{2+}$ ion can, although not nearly as well as $Cu^{2+}$.

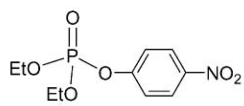

**6**

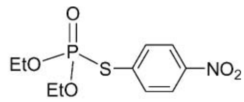

**7**

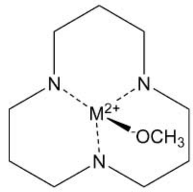

**8**

Indeed, as little as 1 mM of the $Cu^{2+}(^-OCH_3)$ complex of 1,5,9-triazacyclododecane (**8**, M = Cu), catalyzes[4] the methanolysis of **3** at near neutral $^{s}_{s}$pH (8.75)[5,6] with a $t_{1/2}$ of *ca.* 57 s accounting for an $8.4 \times 10^8$-fold acceleration relative to the background reaction.

In an effort to ascertain whether the non-oxime metallacycles (**1**) described by Ryabov, Kazankov and co-workers[1] can promote the methanolysis of P=S pesticides as efficiently as does the $Cu^{2+}(^-OCH_3)$ complex **8**, we prepared the benzyldimethylamine

DOI: 10.1039/b508917d

pyridine trifluoromethanesulfonate palladacycle complex **9** (Pd(dmba)(py)(OTf)), and studied its catalysis of the methanolysis of fenitrothion and the related P=S pesticides **4**, **5**, **10** (coumaphos) and **11** (dichlofenthion). The following represents our findings in this project.

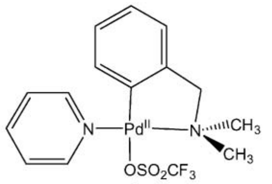

**9**

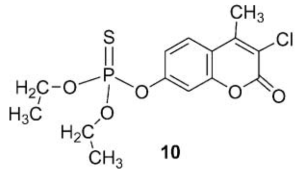

**10**

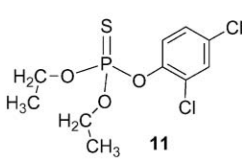

**11**

## Experimental

### (a) Materials and methods

Methanol (99.8% anhydrous), sodium methoxide (0.5 mol dm$^{-3}$ solution in methanol) and silver triflate (AgOTf) and paraoxon **6** were purchased from Aldrich and used without further purification. $HClO_4$ (70% aqueous solution) was purchased from BDH. Fenitrothion (**3**, *O*,*O*-dimethyl *O*-(3-methyl-4-nitrophenyl) phosphorothioate), diazinon (**4**, *O*,*O*-diethyl *O*-(2-isopropyl-4-methyl-6-pyrimidinyl) phosphorothioate) and quinalphos (**5**, *O*,*O*-diethyl *O*-(2-quinoxalyl) phosphorothioate) were gifts from Professor Erwin Buncel and Professor Gary van Loon of this department. Phosphorothioate **7** was synthesized by a slight modification of the reported procedure[7] from 4-nitrophenylthiol. Coumaphos (**10**, *O*-(3-chloro-4-methyl-2-oxo-2*H*-chromen-7-yl) *O*,*O*-diethyl phosphorothioate) and dichlofenthion (**11**, *O*,*O*-diethyl *O*-(2,4-dichlorophenyl) phosphorothioate) were purchased from Chem Service Inc.

**Caution:** all of the phosphorus substrates described herein are acetylcholinesterase inhibitors: compounds **3**, **4**, **5**, **10**, and **11** have oral $LD_{50}$ values of 250, 66, 62, 16, and 270 mg kg$^{-1}$ in rats[8] respectively.

$^1$H NMR and $^{31}$P NMR spectra were determined at 400 MHz and 161.97 MHz using a Bruker Avance-400 NMR spectrometer. $^1$H NMR spectra were referenced to the $CD_2H$ peak of $d_4$-methanol appearing at $\delta$ 3.31. $^{31}$P NMR spectra were referenced to an external standard of 70% phosphoric acid in water, and up-field chemical shifts are negative. Elemental analyses were performed by Canadian Microanalytical Service Ltd., Delta, British Columbia, Canada. Mass spectra were determined using a VG Quattro mass spectrophotometer equipped with an electrospray source. IR spectra were obtained on thin films or NaBr pellets and melting points were measured on a Fisher-Johns melting point apparatus.

### (b) Preparation of Pd(dmba)(py)(OTf) complex (9)

Complex **9** was prepared from the monomeric complex Pd(dmba)(py)(Cl) (dmba = *N*,*N*-dimethylbenzylamine), itself being prepared according to the literature procedure[9] and purified through recrystallization from a hexanes–$CH_2Cl_2$ mixture. To a solution of 98.6 mg of the Pd(dmba)(py)(Cl) complex (0.278 mmol) in dichloromethane (20 ml) was added solid AgOTf (89.2 mg, 0.347 mmol). The mixture was stirred at room temperature for 3 h and then filtered through Celite. The Celite was washed with another 10 ml of dichloromethane and the combined organic layers stripped of solvent by rotary evaporation under reduced pressure. The pale white solid residue was recrystallized from a mixture of hexanes and dichloromethane to afford 120.0 mg of crystals, yield 92.3%.

IR (KBr, cm$^{-1}$): 2916 (m), 1603 (s), 1448 (vs), 1306 (vs), 1261 (vs), 1158 (vs), 1029 (vs), 1017 (vs), 843 (m), 740 (m), 630 (m), 514 (m). Mp: 199 °C. $^1$H-NMR (ppm, 400 MHz, $d_4$-methanol): $\delta$ 8.94 (d, $J$ = 8.0 Hz, 2H), 8.15 (t, $J$ = 8.0 Hz, 1H), 7.69 (m, 2H), 7.02 (m, 2H), 6.73 (t, $J$ = 8.0 Hz, 1H), 5.92 (d, $J$ = 8.0 Hz, 1H), 4.08 (s, 2H), 2.83 (s, 6H). $^{19}$F-NMR (ppm, 376.47 MHz, $d_4$-methanol): $\delta$ 80.57. MS (FAB): $m/z$ 319.09 (M − OTf). Anal. calc. for $C_{15}H_{15}N_2F_3O_3PdS$: C 38.60, H 3.24, N 6.00%. Found: C 38.14, H 3.57, N 5.96%.

### (c) X-Ray crystal structure determination

Crystals of **9** and its chloride precursor suitable for diffraction measurements were prepared by recrystallization from a mixture of n-hexane and dichloromethane. A single crystal of each was mounted on a glass fiber with grease and cooled to −93 °C in a stream of nitrogen gas controlled with a Cryostream Controller 700. Data collection was performed on a Bruker SMART CCD 1000 X-ray diffractometer with graphite-monochromated Mo Kα radiation ($\lambda$ = 0.71073 Å), operating at 50 kV and 30 mA over $2\theta$ ranges of *ca.* 4.60–56.62°. No significant decay was observed during the data collection.

Data were processed using the Bruker AXS Crystal Structure Analysis Package, Version 5.10.[10] Neutral atom scattering factors were taken from Cromer and Waber.[11a] The raw intensity data were integrated using the program SAINT-Plus, which corrects for *Lp* and decay. Absorption corrections were applied using the program SADABS.[11b]

Given in Table 1 are the structural data for the data collection and refinement for **9** and its precursor chloride complex Pd(dmba)(py)(Cl), which was obtained by the same procedure. In Table 2 are presented selected bond lengths, bond angles and torsional angles for the two complexes. An ORTEP diagram of **9** at the 50% probability level is given in Fig. 1. Full structural details for each complex are given as ESI.†

CCDC reference numbers (CCDC 278462 and 278463). See http://dx.doi.org/10.1039/b508917d for crystallographic data in CIF or other electronic format.

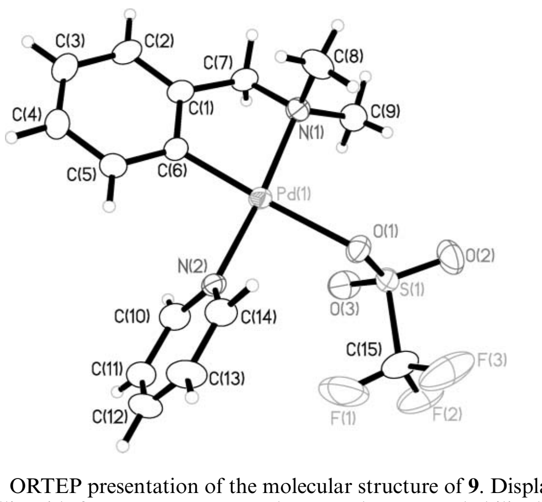


**Fig. 1** ORTEP presentation of the molecular structure of **9**. Displacement ellipsoids for non-H atoms are shown at the 50% probability level and H atoms are represented by circles of arbitrary size.

### (d) Kinetic and titrimetric methods

The $CH_3OH_2^+$ concentration was determined using a Radiometer Vit 90 Autotitrator equipped with a Radiometer GK2322 combination (glass/calomel) electrode calibrated with Fisher Certified Standard aqueous buffers (pH = 4.00 and 10.00) as described in our recent papers.[2,4,12,13] Values of $^s_s$pH were calculated by subtracting a correction constant of −2.24 from the experimental meter reading as reported by Bosch *et al.*[6]

**Table 1** Experimental data for the X-ray diffraction study on complex **9** and its chloride precursor Pd(dmba)(py)(Cl)

| Parameter | Pd(dmba)(py)(OTf) (**9**) | Pd(dmba)(py)(Cl) |
|---|---|---|
| Formula | $C_{15}H_{17}F_3N_2O_3PdS$ | $C_{14}H_{17}ClN_2Pd$ |
| Formula weight | 468.77 | 355.15 |
| $T$/K | 180(2) | 180(2) |
| $\lambda$/Å | 0.71073 | 0.71073 |
| Space group | $P2_1/c$ | *Pbca* |
| Crystal system | Monoclinic | Orthorhombic |
| $a$/Å | 9.1402(17) | 9.5463(18) |
| $b$/Å | 12.351(2) | 16.258(4) |
| $c$/Å | 5.852(3) | 18.117(4) |
| $\alpha$/° | 90 | 90 |
| $\beta$/° | 97.942(3) | 90 |
| $\gamma$/° | 90 | 90 |
| $V$/Å$^3$ | 1772.3(6) | 2811.7(11) |
| $Z$ | 4 | 8 |
| $\rho$/g cm$^{-3}$ | 1.757 | 1.678 |
| $\mu$/mm$^{-1}$ | 1.211 | 1.493 |
| $F$(000) | 936 | 1424 |
| Crystal size/mm | 0.5 × 0.06 × 0.06 | 0.5 × 0.2 × 0.1 |
| $\theta$ range/° | 2.10–28.31 | 2.25–28.28 |
| Index ranges | $-10 \leqslant h \leqslant 12$ | $-12 \leqslant h \leqslant 12$ |
| | $-16 \leqslant k \leqslant 16$ | $-19 \leqslant k \leqslant 21$ |
| | $-20 \leqslant l \leqslant 20$ | $-23 \leqslant l \leqslant 24$ |
| Reflections collected | 11 759 | 18 463 |
| Independent reflections | 4005 ($R_{int}$ = 0.0290) | 3377 ($R_{int}$ = 0.0478) |
| Data/restraints/parameters | 4005/0/294 | 3377/0/231 |
| Goodness-of-fit on $F^2$ | 1.041 | 0.928 |
| Final $R$ indices [$I > 2\sigma(I)$] | $R_1$ = 0.0300, $wR_2$ = 0.0601 | $R_1$ = 0.0329, $wR_2$ = 0.0595 |
| Largest diff. peak and hole/e Å$^{-3}$ | 0.685 and −0.645 | 0.984 and −0.630 |

**Table 2** Selected bond lengths (Å), bond angles (°) and torsion angles (°) for Pd(dmba)(py)(OTf) (**9**) and Pd(dmba)(py)(Cl)

| Parameter | Pd(dmba)(py)(OTf) | Pd(dmba)(py)(Cl) |
|---|---|---|
| Pd(1)–C(6) | 1.958(3) | 1.987(3) |
| Pd(1)–N(2) | 2.035(2) | 2.043(2) |
| Pd(1)–N(1) | 2.075(2) | 2.082(2) |
| Pd(1)–O(1) or Pd(1)–Cl(1) | 2.212(2) | 2.4312(9) |
| C(6)–Pd(1)–N(2) | 92.50(10) | 94.20(12) |
| C(6)–Pd(1)–N(1) | 82.78(10) | 81.95(12) |
| N(2)–Pd(1)–N(1) | 175.20(9) | 176.05(10) |
| C(6)–Pd(1)–O(1) or C(6)–Pd(1)–Cl(1) | 175.89(9) | 175.51(9) |
| N(2)–Pd(1)–O(1) or N(2)–Pd(1)–Cl(1) | 89.22(8) | 89.51(7) |
| N(1)–Pd(1)–O(1) or N(1)–Pd(1)–Cl(1) | 95.55(9) | 94.30(7) |
| C(6)–Pd(1)–N(2)–C(10) | 70.0(2) | −55.4(3) |
| N(1)–Pd(1)–N(2)–C(10) | 60.2(2 | −68.5(3) |
| Cl(1)–Pd(1)–N(2)–C(14) or O(1)–Pd(1)–N(2)–C(14) | 67.9(2) | −51.0(2) |
| Pd(1)–O(1)–S(1)–C(15) | 122.4(2) | |

**(i) Spectrophotometric titration.** A stock solution was prepared by dissolving 4.0 mg of **9** in 1.71 ml of anhydrous methanol and a 0.025 ml aliquot of this was diluted to 2.5 ml through the addition of a 1.0 mmol dm$^{-3}$ $LiClO_4$ in methanol solution such that the final [**9**] = 5 × 10$^{-5}$ mol dm$^{-3}$. The ${}^s_s$pH of the resulting solution was adjusted by addition of aliquots of (0.125–1.25) × 10$^{-3}$ mol dm$^{-3}$ solutions of NaOMe, the ${}^s_s$pH measured and the UV/visible spectra recorded from 220–450 nm.

**(ii) Kinetics.** The kinetics of methanolysis of **3** promoted by [**9**] were monitored as a function of ${}^s_s$pH by observing the rate of appearance of 3-methyl-4-nitrophenol at 318 nm or of 3-methyl-4-nitrophenolate at 404 nm using an OLIS-modified Cary 17 UV/visible spectrophotometer. All reactions were followed to at least three half-times at 25 ± 0.1 °C under buffered conditions. Buffers were prepared from *N*-methylmorpholine (${}^s_s$p$K_a$ = 8.23), trimethylamine (${}^s_s$p$K_a$ = 9.60), triethylamine (${}^s_s$p$K_a$ = 10.78), and 2,2,6,6-tetramethylpiperidine (${}^s_s$p$K_a$ = 11.86). The total [buffer] varied between (1 and 3) × 10$^{-3}$ mol dm$^{-3}$ and the buffers were partially neutralized with 70% $HClO_4$. To avoid any chloride ion contamination from the glass electrode that might affect the metal ion reactions, duplicate solutions were prepared, one for ${}^s_s$pH measurements, and the second portion being used for kinetics. In all cases, ${}^s_s$pH values measured before and after reaction were consistent to within 0.1 units.

The pseudo-first-order rate constants ($k_{obs}$) were evaluated by fitting the absorbance *vs.* time traces to a standard exponential model. The stock solution of the palladium complex (**9**) was prepared in pure methanol at 1 × 10$^{-3}$ mol dm$^{-3}$. In order to determine the kinetic order in [**9**], a series of kinetic runs was undertaken at ${}^s_s$pH 11.54 (2,2,6,6-tetramethylpiperidine buffer) using 2 × 10$^{-5}$ mol dm$^{-3}$ fenitrothion in the presence of varying [complex] from (0.4 to 4) × 10$^{-5}$ mol dm$^{-3}$. The pseudo-first-order rate constants ($k^{obs}_{max}$) given in Table 3 were obtained by extrapolating to a [buffer] = 0.0 mol dm$^{-3}$ and when plotted against [**9**] gave a straight line, the gradient of which was taken as the second-order catalytic rate constant ($k^{obs}_2$). The ${}^s_s$pH dependence of the catalytic rate constant was determined by obtaining the $k^{obs}_{max}$ pseudo-first-order rate constants for the methanolysis of 2 × 10$^{-5}$ mol dm$^{-3}$ fenitrothion between ${}^s_s$pH 8.2 and 12.2 in the presence of a single concentration of **9** (2.0 × 10$^{-5}$ mol dm$^{-3}$). The $k^{obs}_2$ second-order rate constants given in Table 4 and plotted in Fig. 2 were obtained as $k^{obs}_{max}$/[**9**].

**Table 3** Concentration dependence for the pseudo-first-order rate constant of the methanolysis of **3** promoted by **9** and corrected for buffer effects at [**3**] = 2.0 × $10^{-5}$ mol $dm^{-3}$, ${}^s_s$pH 11.54, 2,2,6,6-tetramethylpiperidine buffer, 25 °C

| [**9**]/mol $dm^{-3}$ (× $10^5$) | $k^{obs}_{max}$/$s^{-1}$ [a,b] |
|---|---|
| 4.0 | (1.23 ± 0.01) × $10^{-1}$ |
| 3.0 | (1.04 ± 0.05) × $10^{-1}$ |
| 2.0 | (6.80 ± 0.08) × $10^{-2}$ |
| 1.6 | (5.56 ± 0.07) × $10^{-2}$ |
| 1.2 | (4.93 ± 0.07) × $10^{-2}$ |
| 0.8 | (2.77 ± 0.07) × $10^{-2}$ |
| 0.4 | (8.73 ± 0.66) × $10^{-3}$ |

[a] Rate constants determined at three different [buffer] from (1–3) × $10^{-3}$ mol $dm^{-3}$, and extrapolated to zero [buffer]. [b] Errors are calculated from the standard deviation of the mean.

**Table 4** Observed maximal pseudo-first-order rate constants ($k^{obs}_{max}$) for the methanolysis of **3** catalyzed by **9** at [**3**] = 2.0 × $10^{-5}$ mol $dm^{-3}$, [**9**] = 2.0 × $10^{-5}$ mol $dm^{-3}$, 25 °C as a function of ${}^s_s$pH[a]

| ${}^s_s$pH (amine buffer) | $k^{obs}_{max}$/$s^{-1}$ [b] |
|---|---|
| 8.22 (*N*-methylmorpholine) | (1.86 ± 0.15) × $10^{-4}$ |
| 8.54 (*N*-methylmorpholine) | (4.48 ± 0.23) × $10^{-4}$ |
| 9.05 (trimethylamine) | (9.80 ± 0.20) × $10^{-4}$ |
| 9.54 (trimethylamine) | (3.21 ± 0.15) × $10^{-3}$ |
| 10.23 (trimethylamine) | (1.65 ± 0.04) × $10^{-2}$ |
| 10.49 (triethylamine) | (2.09 ± 0.05) × $10^{-2}$ |
| 10.87 (triethylamine) | (3.76 ± 0.09) × $10^{-2}$ |
| 11.29 (triethylamine) | (6.86 ± 0.07) × $10^{-2}$ |
| 11.49 (2,2,6,6-tetrapiperidine) | (6.82 ± 0.10) × $10^{-2}$ |
| 11.91 (2,2,6,6-tetrapiperidine) | (7.99 ± 0.32) × $10^{-2}$ |
| 12.23 (2,2,6,6-tetrapiperidine) | (8.17 ± 0.55) × $10^{-2}$ |

[a] Observed second-order rate constants ($k^{obs}_2$) are computed as $k^{obs}_{max}$/2 × $10^{-5}$ mol $dm^{-3}$ and are plotted in Fig. 3 against ${}^s_s$pH. [b] Errors are calculated from the standard deviation of the mean of duplicate runs.

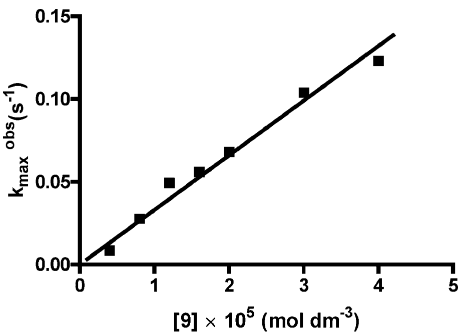


**Fig. 2** Plot of $k_{max}$ *vs.* [**9**] for the methanolysis of **3** (2.0 × $10^{-5}$ mol $dm^{-3}$) at 25 °C, buffer 2,2,6,6-tetrapiperidine (1–3) × $10^{-3}$ mol $dm^{-3}$, extrapolated to zero [buffer], ${}^s_s$pH 11.54. Maximal second-order rate constant ($k^{max}_2$) for catalyzed reaction from the gradient of the plot is (3.30 ± 0.11) × $10^3$ $dm^3$ $mol^{-1}$ $s^{-1}$.

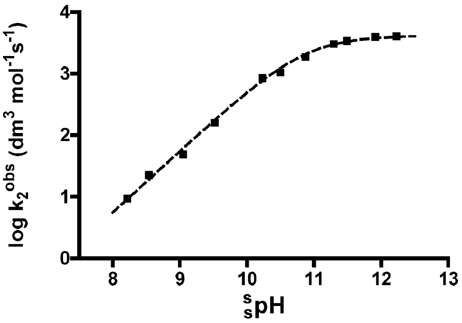


**Fig. 3** Plot of log $k^{obs}_2$ *vs.* ${}^s_s$pH for the methanolysis of **3** at [**3**] = 2.0 × $10^{-5}$ mol $dm^{-3}$, catalyzed by **9** ([**9**] = 2.0 × $10^{-5}$ mol $dm^{-3}$) at 25 °C. The line through the data computed from the fit to eqn. (2), gives a $k^{max}_2$ of 4.13 × $10^3$ $dm^3$ $mol^{-1}s^{-1}$, and a kinetic ${}^s_s$p$K_a$ of 10.87.

The kinetics of methanolysis of substrates **6** and **7** were also studied at ${}^s_s$pH 10.80. The concentration of **9** for these determinations was set at (0.2 to 1) × $10^{-3}$ mol $dm^{-3}$, substrate **6** was set at 2 × $10^{-5}$ mol $dm^{-3}$ and substrate **7** at 4.03 × $10^{-5}$ mol $dm^{-3}$, respectively.

**(iii) NMR turnover experiments.** Catalytic turnover of the methanolysis of an excess of substrates **3**, **4**, **5**, **10**, and **11** relative to [**9**] was investigated using $^1$H and $^{31}$P NMR at ${}^s_s$pH 10.80 under buffered conditions. A typical experiment is described for diazinon. To 0.35 ml of triethylamine buffer (0.1 mol $dm^{-3}$, ${}^s_s$pH 10.80) and 0.27 ml of $d_4$-methanol (added as an NMR lock signal) was added 0.070 ml of a stock solution of 4.0 × $10^{-2}$ mol $dm^{-3}$ diazinon (**4**) in methanol. To the resulting mixture was added 0.020 ml of a 1.05 × $10^{-2}$ mol $dm^{-3}$ stock solution of **9**. At this point, the concentration of **4** was 3.9 × $10^{-3}$ mol $dm^{-3}$ and that of **9** was 2.9 × $10^{-4}$ mol $dm^{-3}$ ([**4**]/[**9**] = 13.4). The kinetics were followed by determining the rate of loss of the diazinon $^1$H NMR signal at 6.82 ppm and the rate of increase of the product 2-isopropyl-6-methylpyrimidin-4-olate signal at 6.10 ppm, the general time course for these being shown in Fig. 4. Independent fitting of the two sets of intensity *vs.* time data to a standard exponential model gave the pseudo-first-order rate constant presented in Table 5. The completion of the reaction was also confirmed by $^{31}$P NMR since the signal for diazinon **4** at $\delta$ 60.8 ppm[14] was completely replaced by that of the product *O*,*O*-diethyl *O*-methyl phosphorothioate at $\delta$ 69.70 ppm (lit.[15] $\delta$ 69.85).

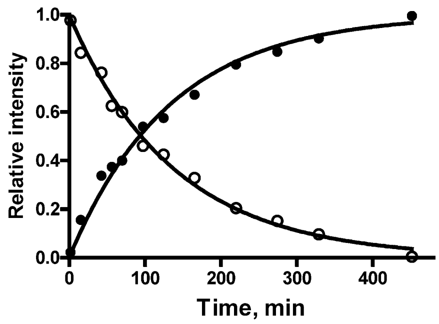


**Fig. 4** Turnover experiment for the methanolysis of diazinon **4** (3.9 × $10^{-3}$ mol $dm^{-3}$) in the presence of **9** (2.9 × $10^{-4}$ mol $dm^{-3}$), $CH_3OH$–$CD_3OD$ (3 : 2), 0.05 M TEA buffer (${}^s_s$pH = 10.80) monitored by $^1$H NMR. Open circles (○) = disappearance of $\delta$ 6.83 ppm signal of **4**; filled circles (●) = appearance of $\delta$ 6.10 ppm signal attributable to 2-isopropyl-6-methylpyrimidin-4-olate product.

NMR turnover experiments for the rate of methanolysis of **3** (stock solution 7.3 × $10^{-2}$ mol $dm^{-3}$), **5** (stock solution 4.0 × $10^{-2}$ mol $dm^{-3}$), **10** (stock solution 2.8 × $10^{-2}$ mol $dm^{-3}$), and **11** (stock solution 7.3 × $10^{-2}$ mol $dm^{-3}$) promoted by **9** were conducted in the same way as with **4** by injecting 70 µl of the various stock solutions into buffered $d_4$-methanol along with 10 µl (for **3**, **10** and **11**) or 20 µl (for **5**) of the stock solution of **9**. The $^1$H and $^{31}$P NMR data for the substrates and corresponding products are listed in Table 6, while the kinetic constants and turnover numbers are listed in Table 5.

## Results

### (a) Kinetics of methanolysis of 3

**(i) Preliminary experiments.** In preliminary experiments to determine the propensity of **9** to catalyze the methanolysis of fenitrothion **3**, we attempted to use phenol buffers such as pentafluorophenol (${}^s_s$p$K_a$ = 9.24),[2] 2,3,5-trichlorophenol (${}^s_s$p$K_a$ = 10.64)[2b] and 2,5-dichlorophenol (${}^s_s$p$K_a$ = 11.06),[2b] but each of these exhibits strong inhibition of the catalysis presumably through binding to the metal complex. Amine buffers such as *N*-methylmorpholine, trimethylamine, triethylamine and 2,2,6,6-tetramethylpiperidine (${}^s_s$p$K_a$ values given in the Experimental

**Table 5** $^1H$ NMR turnover conditional rate constants for the methanolysis of different phosphorothioate esters catalyzed by **9** at 0.05 mol dm$^{-3}$ TEA, pH 10.8, 25 °C

| Phosphorothioate esters/mol dm$^{-3}$ | | TON | $k^{obs}/s^{-1}$ | $k_2^{obs}/dm^3\ mol^{-1}\ s^{-1}$ |
|---|---|---|---|---|
| **3** | $7.3 \times 10^{-3}$ | 48.6 | $(5.35 \pm 0.6) \times 10^{-3}$ | 36.9[a] |
| **4** | $3.9 \times 10^{-3}$ | 13.4 | $(1.30 \pm 0.1) \times 10^{-4}$ | 0.45[b] |
| **5** | $3.9 \times 10^{-3}$ | 13.4 | $(3.53 \pm 0.3) \times 10^{-5}$ | 0.12[b] |
| **10** | $2.8 \times 10^{-3}$ | 18.6 | $>2.2 \times 10^{-2}$ | >146.7[a] |
| **11** | $7.3 \times 10^{-3}$ | 48.6 | $(6.65 \pm 0.3) \times 10^{-3}$ | 44.3[a] |

[a] [9] = $1.5 \times 10^{-4}$ mol dm$^{-3}$. [b] [9] = $2.9 \times 10^{-4}$ mol dm$^{-3}$.

**Table 6** NMR spectral data of the turnover experiment for the methanolysis of different phosphorothioate esters catalyzed by **9** at 0.05 M TEA, $CH_3OH$–$CD_3OD$ (3 : 2), pH 10.80, 25 °C

| | $^1H$ NMR (aromatic protons), $\delta$/ppm | | $^{31}P$ NMR, $\delta$/ppm | |
|---|---|---|---|---|
| Substrate | Substrate | Product | Substrate | Product |
| **3** | 8.04 (1H), 7.21 (2H) | 7.98 (1H), 6.58 (2H) | 66.18 | 73.29[a] |
| **4** | 6.82 (1H) | 6.10 (1H) | 60.76 | 69.70[b] |
| **5** | 8.69 (1H), 8.12 (1H), 7.98 (1H), 7.85 (2H) | 8.20 (1H), 7.84 (1H), 7.59 (1H), 7.37 (2H) | 61.57 | 69.70[b] |
| **10** | 7.85 (1H), 7.26 (2H) | 7.58 (1H), 6.79 (1H), 6.63 (1H) | 62.73 | 69.67[b] |
| **11** | 7.54 (1H), 7.35 (2H) | 7.27 (1H), 7.07 (1H), 6.84 (1H) | 63.29 | 69.60[b] |

[a] Authentic product *O*,*O*,*O*-trimethyl phosphorothioate reported[15] $^{31}P$ NMR $\delta$ 73.40 ppm. [b] Authentic product *O*,*O*-diethyl *O*-methyl phosphorothioate reported[15] $^{31}P$ NMR $\delta$ 69.85 ppm.

section) were found to inhibit the catalysis far less, but to obtain the accurate $k_{obs}$ constants at [buffer] = 0 mol dm$^{-3}$, the kinetics were always measured at 1, 2 and 3 mmol dm$^{-3}$ buffer concentrations and the buffer-independent catalytic rate constant ($k_{max}^{obs}$) was determined either from linear extrapolations (at lower pH) or curve fittings (at higher pH) of the plots of $k_{obs}$ *vs.* [buffer] to zero buffer.

Methanol stock solutions of **9** in the absence of buffer are stable for at least 10 d. The stability of **9** was also checked at ${}^s_s$pH 10.54 and the same activity was demonstrated over at least 500 min, which is a time period sufficient for any of the kinetic experiments described here. Above ${}^s_s$pH 11.00, the complex exhibits some ageing process which diminished its activity, but we did not investigate this process in any detail other than to determine the kinetics under conditions where the ageing was minimal. The catalyzed reaction is also inhibited by the presence of $Cl^-$. We started the catalytic study with the chloride complex Pd(dmba)(py)(Cl), but it immediately became clear that at higher concentrations of catalyst there was an inhibitory effect suggestive of dissociated $Cl^-$ attaching itself to the $Pd^{II}$ preventing access of the methoxide or substrate, both of which are required for the catalysis. Further experiments (not shown) using $1 \times 10^{-5}$ mol dm$^{-3}$ of fenitrothion in the presence of $2 \times 10^{-4}$ mol dm$^{-3}$ Pd(dmba)(py)(OTf) and $1 \times 10^{-4}$ mol dm$^{-3}$ $NaOCH_3$ (${}^s_s$pH 11.50) with varying [n-$Bu_4$Cl] showed asymptotic reduction in the $k_{obs}$ *vs.* [$Cl^-$] plots suggestive of a one site inhibition with $K_{inhibition} = (1.1 \pm 0.1) \times 10^{-3}$ mol dm$^{-3}$. Owing to the inhibitory effect of $Cl^-$, all of the following catalytic studies used Pd(dmba)(py)(OTf) (**9**).

**(ii) Dependence of the kinetic values for the methanolysis of 3 on [9] and ${}^s_s$pH.** The concentration dependence for the methanolysis of **3** was initially measured at ${}^s_s$pH 11.54 (2,2,6,6-tetramethylpiperidine buffer) with the $k_{max}^{obs}$ values being given in Table 3 and plotted in Fig. 2. The plot is linear, indicative of the kinetically active monomeric form of **9**. The second rate constant ($k_2^{obs}$) is evaluated as the gradient of the linear plot, $(3.30 \pm 0.11) \times 10^3$ dm$^3$ mol$^{-1}$ s$^{-1}$.

The pseudo-first-order rate constants ($k_{max}^{obs}$) for the methanolysis of **3** promoted by a $2.0 \times 10^{-5}$ mol dm$^{-3}$ solution of **9** at 11 different ${}^s_s$pH values between ${}^s_s$pH 8.22 and 12.23 are presented in Table 4. The corresponding second-order rate constants, $k_2^{obs}$, are obtained as $k_{max}^{obs}/(2 \times 10^{-5}$ mol dm$^{-3}$) and are plotted in Fig. 3. The appearance of the plot suggests a catalytic process where a basic form of the catalyst is active as in eqn. (1), from which can be derived the kinetic expression given in eqn. (2). NLLSQ fitting of the data gives a $k_2^{max}$ of $4.13 \times 10^3$ dm$^3$ mol$^{-1}$ s$^{-1}$ and a kinetic ${}^s_s$p$K_a$ of 10.8 ± 0.1, the best fit line through the data also being shown in Fig. 3.

$$\mathrm{L:Pd^+{:}OTf^- + HOCH_3 \rightleftharpoons {}^-OTf + L:Pd^+:HOCH_3} \xrightleftharpoons[K_a]{-H^+} \mathrm{L:Pd:{}^-OCH_3} \xrightarrow[k_2^{max}]{3} \mathrm{P} \quad (1)$$

$$k_2^{obs} = k_2^{max}(10^{-pK_a}/(10^{-pH} + 10^{-pK_a})) \quad (2)$$

The catalysis of the methanolysis of **3** by palladacycle **9** is such that one can calculate that a 1 mmol dm$^{-3}$ solution of **9**, at ${}^s_s$pH values of 9.05 and 12.3, gives $t_{1/2}$ values for methanolysis of **3** of 13.0 s and 166 ms respectively.

**(b) Spectrophotometric titration of 9**

As a function of increasing ${}^s_s$pH, the UV spectrum of **9** in methanol has an absorbance increase at 252 nm, a decrease at 231 nm and an isosbestic point at 238 nm. The change in absorbance at 231 nm of a $5 \times 10^{-5}$ mol dm$^{-3}$ solution of **9** in methanol as a function of ${}^s_s$pH was fit to eqn. (3) to generate a spectrophotometric ${}^s_s$p$K_a$ of 10.8 ± 0.1, an $Abs_0$ of 0.649 and a ΔAbs of −0.056. The dashed line through the data given in Fig. 5 is constructed on the basis of this fit.

$$Abs = Abs_0 + \Delta Abs(10^{-pK_a}/(10^{-pH} + 10^{-pK_a})) \quad (3)$$

**(c) NMR turnover experiments for the methanolysis of 3, 4, 5, 12 and 13 promoted by 9**

NMR experiments were performed in a 2 : 3 $CD_3OD$–$CH_3OH$ solution containing triethylamine buffer (0.05 mol dm$^{-3}$) at ${}^s_s$pH 10.80, with [**9**] = $(1.5–2.9) \times 10^{-4}$ mol dm$^{-3}$ and the concentrations of substrates **3**, **4**, **5**, **10**, and **11** being $(2.8–7.3) \times 10^{-3}$ mol dm$^{-3}$, affording [phosphorothioate]/[catalyst] ratios of 48.6, 13.4, 13.4, 18.6, and 48.6 respectively (see Table 5). For the slower substrates, the higher concentration of catalyst was used. The rates of the reactions were monitored by $^1H$ NMR by observing the changes in the peak intensities of the appropriate aromatic protons. The completions of the reactions were also verified by $^{31}P$ NMR which showed that each of the

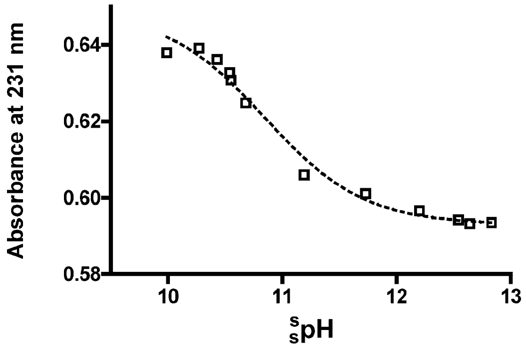


**Fig. 5** Plot of the absorbance of **9** at 231 nm ([**9**] = 5.0 × $10^{-5}$ mol $dm^{-3}$, 1 mmol $dm^{-3}$ $LiClO_4$ in methanol solution, $T$ = 25 °C) as a function of $^s_s$pH showing a spectrophotometric $^s_s$p$K_a$ of 10.8 ± 0.1. Dashed line from fit of the data to eqn. (3).

starting phosphorothioate materials had been replaced by a single methoxylated product.

Listed in Table 6 are the $^1$H NMR starting material and product signals used to determine the kinetics of decomposition of the various substrates under turnover conditions. In all cases, the intensity *vs.* time data adhered to good first-order behaviour for at least three half-times, and standard fitting of the data to an exponential model yielded the pseudo-first-order rate constants given in Table 5 along with the turnover numbers.

### (d) Kinetics of methanolysis of P=O substrates paraoxon (6) and *O*,*O*-diethyl *S*-*p*-nitrophenyl phosphorothioate 7

The methanolyses of these P=O substrates promoted by **9** were very slow, compared with the above P=S counterparts. The absorbance *vs.* time trace for the reaction of paraoxon at $^s_s$pH = 10.80, with [**9**] = 2.0 × $10^{-3}$ mol $dm^{-3}$ and [**6**] = 4.02 × $10^{-5}$ mol $dm^{-3}$, showed no change after 33 h. Assuming that less than 5% of the reaction would have been observable, we set an upper limit for the $k_{obs}$ of 5.3 × $10^{-6}$ $s^{-1}$. Methanolysis of the *S*-*p*-nitrophenyl phosphorothioate derivative **7** (2.0 × $10^{-5}$ mol $dm^{-3}$) at $^s_s$pH = 10.80 promoted by 2.0 × $10^{-4}$ mol $dm^{-3}$ **9** gave an easily monitored reaction, the $k_{obs}$ being 3.83 × $10^{-5}$ $s^{-1}$. Relative to the background methoxide reaction at $^s_s$pH = 10.80,[2b] the acceleration is an unimpressive 236-fold.

## Discussion

### (a) Structure of 9 and its chloride precursor Pd(dmba)(py)(Cl)

The solid state structure of **9** is shown in Fig. 1 with selected structural details, bond lengths and angles being given in Tables 1 and 2 along with those for the chloride precursor whose structure is not shown here but is given in the ESI.† Both structures are very similar to those reported for the analogous Pd(py)Cl oximes[9] in terms of the overall square planar geometry and the bond lengths and angles about the $Pd^{II}$. The triflate in **9** is singly-coordinated to the Pd *trans* to the aryl–Pd with the C(6)–Pd(1)–O(1) angle being 175.89(9)°. The torsional angle between the pyridine plane and the palladium $C_1$ plane is 24.6°. The trifluoromethyl group is tilted toward the pyridine ring with a torsion angle C(15)–S(1)–O(1)–Pd(1) of −122.36(17)°.

### (b) Solution behaviour of 9 as a function of $^s_s$pH

The aqueous solution behaviour of Pd(dmba)(py)(Cl) is reported to involve complete replacement of the Cl with $H_2O$, the latter reported to have a p$K_a$ of 4.18 in water[9,16] to yield the hydroxo-coordinated compound, Pd(dmba)(py)($^-$OH) (**12**). At pH values lower than 3, and greater than 10, the pyridine dissociates from the palladium, presumably due to its protonation at low pH, and through replacement by $HO^-$ at high pH. In the intermediate pH range, Pd(dmba)(py)($^-$OH) was said to be the catalytically active form in promoting the hydrolysis of *p*-nitrophenyl acetate[16] for which the catalytic rate constants plateaued above the p$K_a$ of 4.18. On the other hand, in a later study of the hydrolysis of *N*-*t*-BOC–methionine *p*-nitrophenyl ester promoted by **12**, it was reported[1b] that there was a pronounced [$^-$OH] dependent increase in the $k_{cat}$ values above pH 7.5. Since the proposed mechanism proceeded *via* the *S*-coordinated palladacycle **13**, it was suggested that either the p$K_a$ of the Pd($OH_2$) was shifted markedly upward when coordinated to S, or that the reaction involved attack of external $HO^-$.

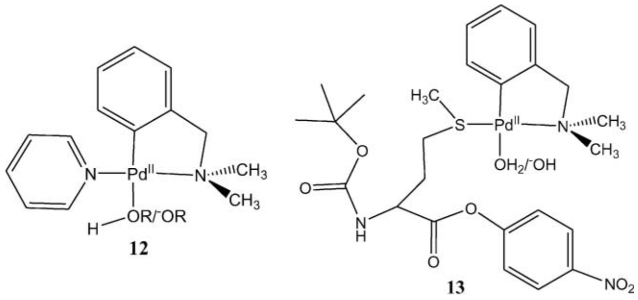


**12** **13**

The behaviour of **9** and its chloride precursor Pd(dmba)(py)(Cl) in methanol solution has both similarities to and differences from the situation in water.[1b,9,16] We assume that the triflate of **9** is completely dissociated in methanol, to give the methanol analogue **12**–$HOCH_3$. Furthermore, we assume that the Cl of Pd(dmba)(py)(Cl) is somewhat less dissociated in methanol to form **12**–$HOCH_3$ due to the fact there is a common ion rate suppression of the latter's catalysis of the methanolysis of fenitrothion. However, we have been unable to detect an ionization event attributable to a low $^s_s$p$K_a$ for the conversion of $Pd^{II}$–$HOCH_3$ to $Pd^{II}$–$^-OCH_3$. For example, the measured $^s_s$pH values of solutions comprising (0.5 to 5) × $10^{-4}$ mol $dm^{-3}$ **9** in methanol are all above neutrality (8.38), being 9.83–10.55 indicating that there is no ionization of $Pd^{II}$–$HOCH_3$ having a low $^s_s$p$K_a$. Additionally, the potentiometric titration profile for a solution of 5.0 × $10^{-4}$ mol $dm^{-3}$ **9** in methanol, containing a sufficient amount of added $HClO_4$ that the starting $^s_s$pH was 3, shows no detectable ionizable protons (outside those for the strong acid region) having a $^s_s$p$K_a$ value of between 3 and 10.

Some indication of the solution behaviour of **9**/**12** as a function of $^s_s$pH is obtained from $^1$H NMR studies of a 6.2 × $10^{-3}$ mol $dm^{-3}$ solution of **9** in $d_4$-methanol under three sets of conditions: (a) immediately after formulation; (b) after the addition of 1 equiv. of neat $HClO_4$; and, (c) after the addition of $NaOCH_3$ to the solution from (a). In Scheme 1 are shown the various species supported by the solution NMR spectra under the above conditions. We have used the characteristic peaks of the pyridine resonances and those of the benzylic $CH_2$ group since they are visibly sensitive to changes in the coordination environment. The $^1$H NMR spectrum of the first solution gives evidence of a single observable material that we assign as palladacycle **12**–$HOCH_3$. As is the reported case in water,[1,9] under acidic conditions some pyridine dissociates from the complex (*ca.* 55% observed by $^1$H NMR), leaving two Pd-containing species in solution as well as some visible precipitate. The species in solution are **12**–$HOCH_3$ (*ca.* 45%, calculated from integration of phenyl and pyridine protons) along with 32% of the palladacycle **14** without an associated pyridine [$^1$H NMR ($\delta$, ppm): *ca.* 7.00, 4H; 3.98, 2H; 2.80 6H]. The latter has a limited solubility in methanol at these concentrations producing some precipitate, but when the isolated precipitate is redissolved in fresh $d_4$-methanol, the product proved to be the same palladacycle without pyridine (**14**).

A second solution containing 7.2 × $10^3$ mol $dm^{-3}$ of **9** was treated with 0.5 equiv. and then a second 0.5 equiv. of NaOMe. After the first addition of base, the $^1$H NMR spectrum gave evidence of the presence of **12**–$HOCH_3$ (signals

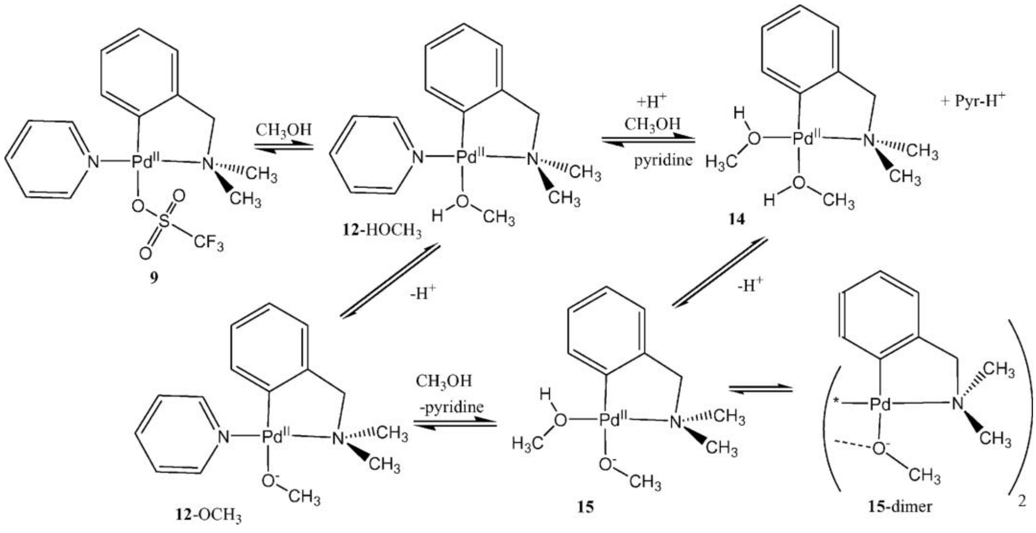


**Scheme 1**

slightly broadened) along with some dissociated pyridine, with considerably broadened resonances, and an equivalent amount of palladacycle having a benzylic resonance at *ca.* 3.86 ppm, and having two distinct N–$CH_3$ resonances at 2.73 and 2.78 ppm. Further addition of base intensified the signals of free pyridine and the latter palladacycle which is probably a composite of at least two forms: **15**–($HOCH_3$)($^-OCH_3$), which itself is in equilibrium with a **15**-dimer, as in Scheme 1. The **12**–$^-OCH_3$ form must be in rapid equilibrium with **12**–$HOCH_3$, but dissociation of pyridine from the former to give **15**–($HOCH_3$)($^-OCH_3$) must be rather slow on the NMR timescale. Since the palladacycle benzylic $CH_2$ resonances and two N–$CH_3$ resonances are fairly sharp, the dominant equilibrium structure probably comprises the **15**-dimer in *syn* and *anti* forms. It is of note that the dimer of the chloride complex $(Pd(dmba)Cl)_2$, when dissolved in $d_4$-methanol containing an excess of $NaOCH_3$, produces a $^1H$ NMR spectrum which is virtually identical to the spectrum of what we propose as the **15**-dimer including the two different intensity N–$CH_3$ resonances, thus supporting the *syn* and *anti* dimers as being the source of the latter resonances.

All of the above indicates that there is no observable dissociation of a proton from the metal-coordinated methanol at low ${}^{s}_{s}pH$. In fact, the spectrophotometric titration of a solution comprising $5 \times 10^{-5}$ mol $dm^{-3}$ of **9** in methanol between ${}^{s}_{s}pH$ 10 and 13 indicates a spectrophotometric ${}^{s}_{s}pK_a$ of 10.85, a value consistent with the kinetic ${}^{s}_{s}pK_a$ discussed below.

### (c) Kinetics of catalyzed methanolysis of 3 promoted by 9

The $k^{obs}$ *vs.* concentration plot for the methanolysis of **3** catalyzed by varying [**9**] at ${}^{s}_{s}pH$ 11.4 is linear and the gradient is defined as $k_2^{obs}$. The second-order catalytic rate constants at other ${}^{s}_{s}pH$ values listed in Table 4 were computed from the $k^{obs}$ values obtained at a single concentration of catalyst, and extrapolated to zero buffer concentration to give $k_{max}^{obs}$, with $k_{max}^{obs}$/(catalyst) = $k_2^{obs}$. The log of the $k_2^{obs}$ values, when plotted against ${}^{s}_{s}pH$ as in Fig. 3, and fit to the expression in eqn. (2) gives a kinetic ${}^{s}_{s}pK_a$ of 10.87 and a maximal second-order rate constant of $4.13 \times 10^3$ $dm^3$ $mol^{-1}$ $s^{-1}$. This value can be compared with the second-order rate constant for the same process catalyzed by **8**:$Cu^{2+}$($^-OCH_3$) of 12.2 $dm^3$ $mol^{-1}$ $s^{-1}$.[4] While **9** is apparently more active than **8**:$Cu^{2+}$($^-OCH_3$) by about 300-fold, the latter, owing to its lower ${}^{s}_{s}pK_a$, is about equally as effective at that ${}^{s}_{s}pH$. For example, solutions of 1 mmol $dm^{-3}$ in each catalyst, **8**:$Cu^{2+}$ or **9**, when compared at the same ${}^{s}_{s}pH$ value of 8.75 catalyze the methanolysis of **3** with $t_{1/2}$ values of 57 and 19 s, corresponding to an acceleration over the background reaction of $8.4 \times 10^8$-fold and $4.9 \times 10^9$-fold respectively.

### (d) Turnover experiments

The methanolysis of five P=S pesticides (fenitrothion (**3**), diazinon (**4**), quinalphos (**5**), coumaphos (**10**) and dichlofenthion (**11**)), catalyzed by **9** under turnover conditions was investigated by $^1H$ and $^{31}P$ NMR under buffered conditions (0.05 M triethylamine, ${}^{s}_{s}pH$ 10.80, ambient temperature) in $d_4$-methanol. The particular ${}^{s}_{s}pH$ value and buffer conditions were chosen to match the kinetic and spectroscopic ${}^{s}_{s}pK_a$ values of 10.8, but the conditional rate constants determined from solutions under buffered NMR conditions that are reported in Table 5 are lower than we previously obtained under spectroscopic conditions extrapolated to zero [buffer]. By way of comparison, the $k_2^{obs}$ for the catalyzed methanolysis of **3** under spectroscopic conditions at ${}^{s}_{s}pH$ 10.8 is *ca.* 1880 $dm^3$ $mol^{-1}$ $s^{-1}$, while that obtained from the NMR experiment is some 50-fold lower at 36.9 $dm^3$ $mol^{-1}$ $s^{-1}$. The drop in reactivity is due to the large concentration of inhibitory buffer in the NMR experiment, which is required to control the ${}^{s}_{s}pH$, as well as the larger concentrations of substrate and catalyst which can alter the solution properties. Nevertheless, these are still very effective catalytic systems for the decomposition of these classes of pesticides, capable of forming non-toxic, methoxylated products under turnover conditions with good first-order kinetics and without any product inhibition.

### (e) Conclusions and postulated reaction mechanism

Given in Scheme 2 is a predicted mechanism for the reaction which is consistent with all the available data. The available information suggests that palladacycle **9**, when introduced into methanol solution predominantly exists as a mono-methanol complex ($Pd(dmba)(py)(HOCH_3)$, **12**–$HOCH_3$ in Schemes 1 and 2). The catalytically active form is a basic one (**12**–$^-OCH_3$ and/or **15**) generated by the ionization of a Pd-bound methanol having an ${}^{s}_{s}pK_a$ of 10.8. The mechanism in Scheme 2 is proposed to be an associative one (typical for $Pt^{II}$ and $Pd^{II}$ complexes where steric factors are not large)[17] involving pre-equilibrium binding of the P=S to form a transient five-coordinate complex (**16**) that undergoes intramolecular attack of the coordinated methoxide on P. Whether the reaction involves a stepwise mechanism, through a five-coordinate phosphorane intermediate or *via* concerted displacement of the leaving group, cannot be ascertained on the basis of the available evidence, although we note that the $La^{3+}$- and $Zn^{2+}$-catalyzed methanolysis of phosphate and phosphorothioate triesters was recently shown[2b] to involve concerted displacement of aryloxy leaving groups. Turnover of the catalyst requires displacement of the P=S product from **17**, again probably through an associative process with solvent, followed by deprotonation of the $Pd^{II}$-coordinated methanol.

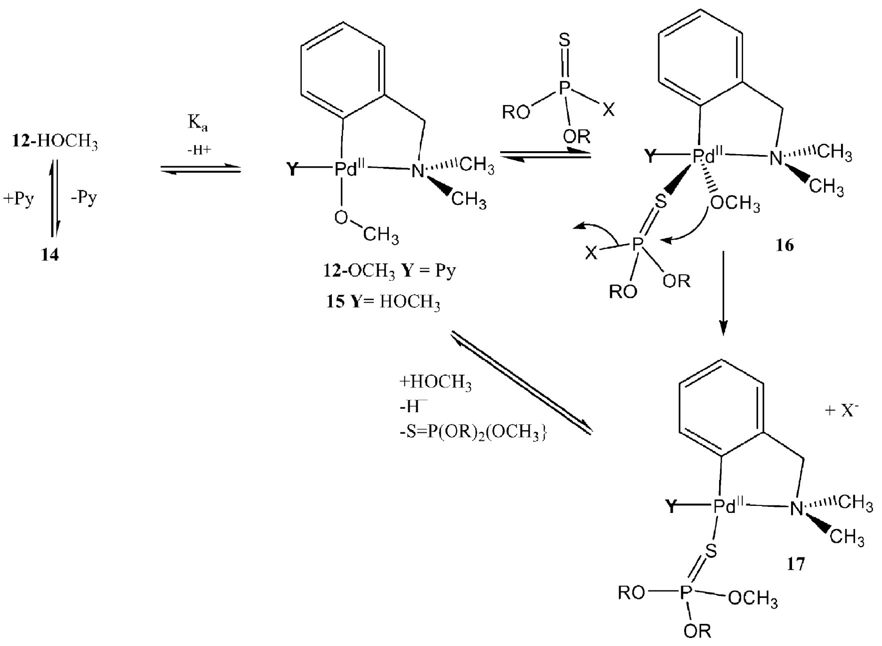


**Scheme 2**

The palladacycle system studied here has some interesting properties that might make it a method of choice for the decomposition of P=S pesticides on larger scale. Since $Pd^{II}$ is considered 'soft' in the Pearson 'hard/soft' sense,[3] the system is selective for P=S-containing organophosphates as is evidenced by the fact that it is ineffective for a typical P=O substrate, paraoxon. It does show some reactivity toward *O*,*O*-diethyl *S*-*p*-nitrophenyl phosphorothioate ($k_2$ = 0.38 dm $mol^{-1}$ $s^{-1}$), but this is less than exhibited by our previously reported[2b] $La^{3+}$ dimer or $Zn^{2+}$:[1,5,9-triazacyclododecane] catalysts, for which the rate constants are 12.4 and 0.84 dm $mol^{-1}$ $s^{-1}$ respectively. Since the reaction medium is methanol the hydrophobic organophosphates and these $Pd^{II}$ catalysts are far more soluble than they are in aqueous solution. Finally, because the reaction is actually a transesterification reaction and not a hydrolysis reaction, the final triester product is neutral and is thus substantially non-inhibitory. While it is true that the $Pd^{II}$ system here is more expensive on a per mole basis than the previous $La^{3+}$ catalysts or the triazacyclodecane $Zn^{2+}(^{-}OCH_3)$ or $Cu^{2+}(^{-}OCH_3)$ systems reported earlier,[2,4] the covalent attachment of the metal to the aryl group and the fact that the catalytic cycle does not involve a $Pd^{II}$ to $Pd^{0}$ redox change suggest that it should be possible to create polymer-bound or solid-supported[18] versions of the catalytic system that can be recovered for re-use. All of the above suggest that further investigation of this class of catalysts should generate practical methods for the destruction of P=S pesticides.

## Acknowledgements

The authors gratefully acknowledge the financial assistance of the Natural Sciences and Engineering Research Council of Canada, Queen's University and the United States Department of the Army, Army Research Office, Grant No. W911NF-04-1-0057 and the Defense Threat Reduction Agency, Joint Science and Technology Office (06012384BP).[19] In addition, we are grateful to Dr Riu-Yao Wang of the Queen's Chemistry X-Ray Structure Determination Laboratory for structure determinations of Pd(dmba)(py)(Cl) and Pd(dmba)(py)(OTf).

## References and notes

1 (*a*) A. D. Ryabov, G. M. Kazankov, S. A. Kurzeev, P. V. Samuleev and V. A. Polyakov, *Inorg. Chim. Acta*, 1998, **280**, 57; (*b*) S. A. Kurzeev, G. M. Kazankov and A. D. Ryabov, *Inorg. Chim. Acta*, 2000, **305**, 1; (*c*) G. M. Kazankov, V. S. Sergeeva, E. N. Efremenko, L. Alexandrova, S. D. Varfolomeev and A. D. Ryabov, *Angew. Chem., Int. Ed.*, 2000, **39**, 3117; (*d*) G. M. Kazankov, V. S. Sergeeva, A. A. Borisenko, A. I. Zatsman and A. D. Ryabov, *Russ. Chem. Bull. Int. Ed.*, 2001, **50**, 1844.
2 (*a*) J. S. Tsang, A. A. Neverov and R. S. Brown, *J. Am. Chem. Soc*, 2003, **125**, 7602; (*b*) T. Liu, A. A. Neverov, J. S. W. Tsang and R. S. Brown, *Org. Biomol. Chem.*, 2005, **3**, 1525; (*c*) J. S. W. Tsang, A. A. Neverov and R. S. Brown, *Org. Biomol. Chem.*, 2004, **2**, 3457; (*d*) W. Desloges, A. A Neverov and R. S. Brown, *Inorg Chem.*, 2004, **43**, 6752.
3 M. B. Smith and J. March, *Advanced Organic Chemistry*, Wiley Interscience, New York, 2001, 5th edn., pp. 338–342 and refs. cited therein.
4 A. A. Neverov and R. S. Brown, *Org. Biomol. Chem.*, 2004, **2**, 2245.
5 For the designation of pH in non-aqueous solvents we use the forms described by Bosch and co-workers[6] based on the recommendations of the IUPAC, in *Compendium of Analytical Nomenclature: Definitive Rules 1997*, Blackwell, Oxford, UK, 1998, 3rd edn. If one calibrates the measuring electrode with aqueous buffers and then measures the pH of an aqueous buffer solution, the term ${}^{w}_{w}$pH is used; if the electrode is calibrated in water and the 'pH' of the neat buffered methanol solution then measured, the term ${}^{s}_{w}$pH is used; and if the electrode is calibrated in the same solvent and the 'pH' reading is made, then the term ${}^{s}_{s}$pH is used.
6 E. Bosch, F. Rived, M. Roses and J. Sales, *J. Chem. Soc., Perkin Trans. 2*, 1999, 1953; F. Rived, M. Rosés and E. Bosch, *Anal. Chim. Acta*, 1998, **374**, 309; E. Bosch, P. Bou, H. Allemann and M. Rosés, *Anal. Chem.*, 1996, **68**, 3651; I. Canals, J. A. Portal, E. Bosch and M. Rosés, *Anal. Chem.*, 2000, **72**, 1802.
7 S.-B. Hong and F. M. Raushel, *Biochemistry*, 1996, **35**, 10 904.
8 *The Merck Index*, Merck & Co. Inc., Rahway, NJ, USA, 1989; *Pesticide and Metabolite Standard Catalogue*, Chem Services Inc., West Chester, Pennsylvania, 2001–2004.
9 A. Ryabov, V. A. Polyakov and A. K. Yatsimirsky, *J. Chem. Soc., Perkin Trans. 2*, 1983, 1503.
10 *Bruker AXS Crystal Structure Analysis Package, Version 5.10 (SMART NT (Version 5.053), SAINT-Plus (Version 6.01), SHELXTL (Version 5.1))*, Bruker AXS Inc., Madison, WI, USA, 1999.
11 (*a*) D. T. Cromer and J. T. Waber, *International Tables for X-Ray Crystallography*, Kynoch Press, Birmingham, UK, 1974, vol. 4, Table 2.2 A; (*b*) G. M. Sheldrick, *SADABS, Program for area detector adsorption correction*, Institute for Inorganic Chemistry, University of Göttingen, Germany, 1996.
12 A. A. Neverov, G. Gibson and R. S. Brown, *Inorg. Chem.*, 2003, **42**, 228.
13 G. Gibson, A. A. Neverov and R. S. Brown, *Can. J. Chem.*, 2003, **81**, 495.

14 R. D. Mortimer and B. A. Dawson, *J. Agric. Food Chem.*, 1991, **39**, 911.
15 S. Ryu, J. A. Jackson and C. M. Thompson, *J. Org. Chem.*, 1991, **56**, 4999.
16 A. K. Yatsimirsky, G. M. Kazankov and A. D. Ryabov, *J. Chem. Soc., Perkin Trans. 2.*, 1992, 1295.
17 M. Schmülling, A. D. Ryabov and R. van Eldik, *J. Chem. Soc., Dalton Trans.*, 1994, 1257; H. Holmann, B. Hellquist and R. van Eldik, *Inorg Chim. Acta*, 1991, **18**, 25.
18 D. E. Bergbreiter, *Chem. Rev.*, 2002, **102**, 3345; D. E. Bergbreiter, P. L. Osburn, A. Wilson and E. M. Sink, *J. Am. Chem. Soc.*, 2000, **122**, 9058; H. P. Dijkstra, M. Q. Slagt, A. McDonald, C. A. Kruithof, R. Kreiter, A. M. Mills, M. Lutz, A. L. Speck, W. Klopper, G. P. M. Van Klink and G. Van Koten, *J. Catal.*, 2005, **229**, 322.
19 The content of the information does not necessarily reflect the position or the policy of the federal government, and no official endorsement should be inferred.